Object watermarking scheme based on resynchronization and shape subdivision

Mei-Yi Wu
Chang Jung Christian University
Department of Information Management
Tainan, Taiwan, R.O.C.
E-mail: barbara@mail.cjcu.edu.tw

Jia-Hong Lee
National Kaohsiung First University of Science and Technology
Department of Information Management
Kaohsiung, Taiwan, R.O.C.

Yu-Kuen Ho
National Cheng Kung University
Department of Electrical Engineering
Tainan, Taiwan, R.O.C.

Abstract. In practical use, objects in still images and videos are easy to misappropriate with handy image-processing tools and need to be protected. However, the few proposals for object watermarking suffer from resynchronization problems. In this study, we develop an object-based watermarking method based on efficient segmentation using lines parallel and perpendicular to two principal axes in the spatial domain. A patch-like scheme is designed to embed and extract invisible watermarks. In contrast with the previous object-based watermarking schemes, extra information for resynchronization is not required to be stored in our method. Experimental results show the robustness of the proposed method against many kinds of geometrical attacks. © *2007 Society of Photo-Optical Instrumentation Engineers.* [DOI: 10.1117/1.2751167]

Subject terms: object-based watermarking; shape subdivision; principal axis; geometrical attacks; resynchronization detection problem; false-positive probability.

Paper 060367RR received May 13, 2006; revised manuscript received Dec. 20, 2006; accepted for publication Jan. 5, 2007; published online Jul. 2, 2007.

1 Introduction

The rapid growth of commercial multimedia services has led to an urgent demand for reliable and secure copyright protection for digital multimedia. Digital watermarking techniques were first introduced in the early 1990s, and are being rapidly developed for various media. In many watermarking applications, watermarks have to survive some expected set of distortions, including digital filtering, lossy compression, analog blurring, addition of random noise, and ghosting. Many robust watermarking techniques, including statistics,[1] signal transformation,[2] spread spectrum,[3] the discrete cosine transform (DCT),[4] the discrete Fourier transform (DFT),[5] wavelets,[6] the Fourier-Mellin transform,[7] fractals,[8] and content-based methods,[9] can be efficiently adopted to add watermarks into digital images. The stego images generated using these schemes can survive common image processing, such as lossy compression, filtering, noise addition, and geometrical transformations. Cox et al.[10] give a comprehensive description of watermarking techniques.

However, geometrical processes like simple rotation, scaling, and translation (RST) are easily performed using certain commercial software such as PhotoImpact and PhotoShop. For this reason, some methods have been proposed to resist RST distortions. Wu et al.[11] and Lin et al.[12] adopt the Fourier-Mellin transform to achieve geometrical-transform invariance. These methods take the whole image into account in embedding and detection processes, though the demand may be for protecting a single object in the image.

Object-based watermarking schemes[13,14] have become more important with the quick developing of the internet and the multimedia standards. Objects in a video frame or pictures on auction Web sites with simple background can easily be separated from their background by using the binary mask provided by the MPEG-4 video format or image-processing tools. Watermark schemes that embed watermarks into a whole image without considering that the image could be misappropriated by removing the background could fail in watermark detection or extraction. Besides, geometrical processes like rotation and skewing could be applied to the usurped object image, making the detection or extraction process more difficult. With cropping and geometrical attacks, watermarks embedded in the media retain most of their original data, but lose the original order and orientation of the embedded data, which are critical for watermark extraction or detection. This problem is called the watermark *resynchronization detection* problem.

With the prevalence of image-processing tools, the resynchronization detection problem is getting more important for the practical use of watermark schemes. Guo and Shi[15] and Lu and Liao[16] recently adopted inertia ellipses and eigenvectors to correct object distortions resulting from geometrical attacks such as rotation and scaling. However, in the method proposed by Guo and Shi, information about the inertia ellipse of the object before watermarking is required for watermark detection. This means that extra information about the inertia ellipse of the original object needs to be recorded for resynchronization. Without the information about the original inertia ellipse, the object cannot be resynchronized to the original dimensions and angular magnitude after the scaling and rotation attacks.

The same situation also happens in the method proposed by Lu and Liao.[16] It is a video object watermarking scheme, based on the concept of communications with side information. Using the eigenvectors of a video object, Lu and Liao's method is able to solve the resynchronization problems caused by geometrical attacks like rotation and

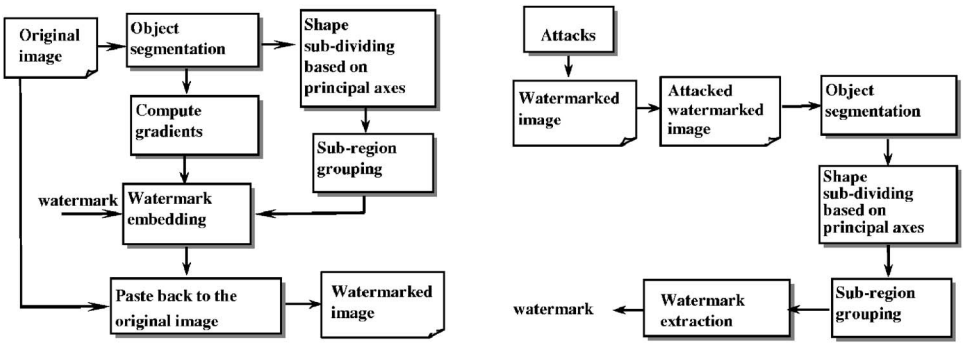

Fig. 1 Block diagram of the proposed watermarking scheme.

flipping. However, embedding watermarks using the DCT coefficients will make this method very sensitive to such attacks. Therefore, the original dimensions and eigenvectors are also needed as extra information in watermark detection for resynchronization.

In our previous work,[17] we have proposed a spatial-domain method based on shape self-similarity segmentation to achieve synchronization detection. This method does not have to record extra information for resynchronization. However, shape self-similarity segmentation is good for convex objects only; it is not general enough for all kinds of object shapes.

To make it general enough for practical applications, we propose an object-based watermarking scheme using a new segmentation algorithm for object images. The proposed method is based on the orientations and lengths of principal axes, and is rotation- and translation-invariant. As long as the principal axes of an object are detected, watermarks embedded in segmented regions can be extracted correctly. In addition, to ensure the reliability of the proposed method, the issue of false positives is discussed in this paper. Figure 1 shows the procedure of the proposed scheme.

The rest of this paper is organized as follows. Section 2 briefly describes the proposed method of segmenting an object image into numerous small subregions. Section 3 then details the procedures of watermark embedding and extraction. Next, Sec. 4 describes experimental results concerning some attacks, including the mean filter, JPEG compression, rotation, rotation and scaling, and geometrical attacks, using the StirMark[18,19] benchmark tool. We also implemented Lu and Liao's[16] method for comparison. Section 5 discusses in detail the experimental results of implemented methods. Conclusions are finally drawn in Sec. 6.

2 The Proposed Shape Subdivision Method for Synchronization

Let f denote an object image segmented from a gray-level or color image, whose corresponding shape S is then obtained in binary image form by transforming all pixel illuminations of f to the same gray value. The shape subdivision corresponding to the principal axes is performed to ensure the success of embedding and extracting operations. This procedure is described as follows:

Step 1: Determine the second-order central moments of S, namely, μ_{02}, μ_{20}, and μ_{11}.

Step 2: Determine the principal angle φ of S from the central moments as

$$\varphi = \frac{1}{2}\tan^{-1}\left(\frac{2\mu_{11}}{\mu_{20}-\mu_{02}}\right). \tag{1}$$

Step 3: Determine the minimum bounding rectangle of the rotated object S with rotation around its mass center c at an angle of φ, so that the length and width of the rectangle are equal to the lengths of computed principal axis and subprincipal axis, respectively.

Step 4: Divide the object image by segmenting the bounded rectangle into $m \times n$ small similar rectangles.

An experiment was conducted using an object image called "Russian Doll" The second-order central moments μ_{02}, μ_{20}, and μ_{11} of this object image are calculated as 1.36×10^8, 2.77×10^8, and -2.457×10^7, respectively. Using these second central moments and Eq. (1), the principal angle φ can be determined. Figure 3a shows the original object image, whose principal angle is obtained as $\varphi = 1.29$ deg. The dimensions of its minimum bounding rectangle are 300×600.

3 Watermark Embedding and Extraction

Suppose that an object image f is divided into $m\times n$ disjoint gray-level image blocks, $B'_1, B'_2, \ldots, B'_{m\times n}$, using the segmentation method mentioned in the preceding section. The parameters m and n can be regarded as secret keys to embed and protect data. All blocks B_i are then split into k groups, $G_1, G_2, \ldots, G_k$, where k denotes the number of bits in the watermark to be embedded. Each group G_i can be denoted as

$$G_i = \left\{ B_j : (i-1)\times\left\lfloor\frac{m\times n}{k}\right\rfloor + 1 \leqslant j \leqslant i\times\left\lfloor\frac{m\times n}{k}\right\rfloor,\ j\in N\right\}. \tag{2}$$

Furthermore, G_i is divided into two subsets C_i and D_i, which contain all the blocks B_j in G_i with odd and even indices, respectively.

Finally, the following is applied to embed the watermark bit w_i:

$$|\bar{C}_i - \bar{D}_i| \geqslant \delta_u \qquad \text{if } w_i = 1,$$

$$|\bar{C}_i - \bar{D}_i| \leqslant \delta_l \qquad \text{if } w_i = 0, \tag{3}$$

where $\overline{C_i}$ and $\overline{D_i}$ denote the means of the pixel intensities of the blocks C_i and D_i, respectively, and δ_u and δ_l represent the upper and lower thresholds to manage the quality of the output watermarked image. The values of $\overline{C_i}$ and $\overline{D_i}$ are adaptively modified by adding or subtracting a fixed value to or from each pixel of the corresponding blocks to fit the requirement of this rule. Additionally, to improve the quality of a watermarked image, the pixel intensities can be adjusted according to the gradient of each pixel to reduce the effect of blockness. The gradient of each pixel computed here is given by

$$g_p = \max_{q \in D}(|p - q|), \tag{4}$$

where D denotes an area centered on pixel p. To avoid the effect of blockness, we adjust the intensity of each pixel according to the capacity of modification, which is given by

$$C_p = \begin{cases} \lfloor \log_2(g_p) \rfloor & \text{if } g_p > 0, \\ 0 & \text{otherwise.} \end{cases} \tag{5}$$

This equation guarantees that a pixel will not be modified if its gradient is very small. Moreover, to blur the boundaries of blocks, 2-D Gaussianlike shape weights can be applied in pixel modification. Equation (5) can be replaced by

$$C_p = \lfloor \log_2(g_p) \rfloor \times \lambda \times \text{Gau\_w}_p, \tag{6}$$

Where λ denotes the strength of the signal, and Gau_w_p is the corresponding weight of pixel p, which is expressed as

$$\text{Gau\_w}_{p(x,y)} = \exp[-d(x,y)/2\sigma^2]. \tag{7}$$

Here $d(x,y)$ is the distance between the pixel $p(x,y)$ and the center of the block in which it is located.

Figure 2 shows an example of the use of these equations to embed a 32-bit watermark into the object image segmented from "Lena." Figure 2(a) is the original object image, Fig. 2(b) is the watermarked image, and Fig. 2(c) shows the 2-D Gaussian shape weights used. Figure 2(b), with high resolution, shows the imperceptibility of proposed method.

To extract watermarks from a test object, the normalization and segmentation procedures performed in the watermark embedding process are performed again with the same specified secret keys. The corresponding blocks can then be calculated, and watermarks can be extracted easily by using $\overline{C_i}$ and $\overline{D_i}$. If $|\overline{C_i} - \overline{D_i}| \geqslant (\delta_u + \delta_l)/2$, then the bit 1 is extracted; otherwise the bit 0 is extracted.

For example, to embed 32 bits into 24×24 blocks, the blocks are split into 18 groups. Each group contains 32 blocks. Then, each group is divided into two subsets for watermark embedding. To embed the watermark, the dimensions of D in Eq. (4) are set to be 2×1, the value of λ in Eq. (5) is 420, and the value of δ, the standard deviation of the 2-D Gaussian, in Eq. (6) is 5.0. The difference of the gray-level values of the two subsets is adjusted to be bigger than a threshold δ_u ($\delta_u = 8$ is used in the experiment shown in Fig. 3) if a watermark bit 1 is embedded. On the other hand, the difference is adjusted to be smaller than δ_l (δ_l

Fig. 2 Proposed scheme applied to a high-resolution object image "Lena." (a) The test object image. (b) The object image in (a) watermarked using the proposed scheme. (c) The 2-D Gaussian weights amplified 20 times for display.

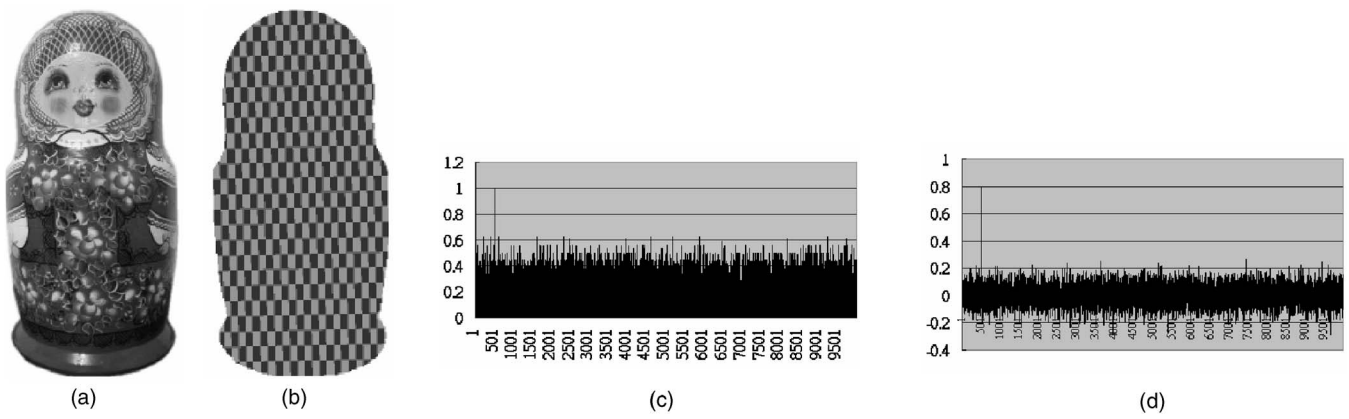

Fig. 3 Proposed scheme applied to the "Russian Doll" object. (a) The test object image. (b) The shape subdivision of the image in (a). (c) The corresponding detector response using the proposed method. (d) The corresponding detector response using Lu and Liao's method.

=2 is used) if a 0 is embedded. Figure 3(b) illustrates the shape segmentation result of dividing Fig. 3(a) into 24 $\times$24 small blocks in which 32 watermark bits were embedded. At the stage of watermark extraction, a bit 1 is extracted if the difference of the sum of gray-level values of two subsets is larger than $(\delta_u+\delta_l)/2$, and a bit 0 is extracted if the difference is smaller than $(\delta_u+\delta_l)/2$.

4 Experimental Results

Experiments were conduced using the object images "Russian Doll," "Vase," "Fish," and "Sea Shell." Some of these object images are neither convex nor symmetric. To evaluate the proposed scheme, two similarity measures, PSNR and NC, are used. The PSNR (peak SNR) is used to measure the gray-image quality, and the NC (normalized correlation) is used to measure the similarity between two bi-level watermarks. The NC[20] is defined as follows:

$$\mathrm{NC} = \frac{\sum_i w_i w_i'}{\sum_i w_i^2} \frac{\sum_i (1-w_i)(1-w_i')}{\sum_i (1-w_i)^2}, \tag{8}$$

where w and w' are two watermark sequences. The NC value is the proportion of the number of watermark bits that have the same value at the same location in both watermark sequences. Different attacks were simulated in these experiments, including mean filtering, JPEG compression, noise, resizing, rotation, and row and column removal.

To evaluate the proposed method, the method proposed by Lu and Liao is implemented for comparison. Their scheme works on an object image in a MPEG-4 video frame, which can be segmented from its background using a binary mask. The scheme can also be applied to embed watermarks into an ordinary still image as long as the object image can be segmented from its background accurately every time we want to process it. Pictures that have simple backgrounds, so that the object can be easily separated from its background (as in most merchandise images found on auction Web sites) are quite proper for this usage. (To make the object more conspicuous to the viewers, pictures on an auction Web site are likely to have a simple background.) The proposed method, like the method proposed by Lu and Liao, can also be used to process object images in an MPEG-4 digital video as well as the object image in an ordinary still image with a simple background.

Since the method proposed by Lu and Liao uses watermark detection, for a proper comparison a watermark detection experiment has been designed. For Lu and Liao's method, 10,000 sets of Gaussian-distributed watermark sequences with zero mean and unit standard deviation are generated. The correlations between the sequences and the watermark extracted from the watermarked image are calculated. For the proposed method, 10,000 sets of randomly generated watermark sequences with equal numbers of 0's and 1's are used to calculate the NC between the random sequence and the watermark extracted from the watermarked image.

Figures 3(a), 4(a), 5(a), and 6(a) show the original object images. The principal angles were obtained as 1.29, 0.1, −11.83, and −7.15 deg for "Russian Doll," "Vase," "Fish," and "Sea Shell," respectively. Figures 3(b), 4(b), 5(b), and 6(b) show the shape segmentation results of dividing original object images into 24$\times$24 small blocks in which 32 watermark bits were going to be embedded. Figures 3(c), 4(c), 5(c), and 6(c) show the corresponding detector response using the proposed method. Figures 3(d), 4(d), 5(d), and 6(d) show the corresponding detector response using Lu's method. The 500th of the 10,000 sequences is replaced with the embedded watermark. From these figures, only one peak exists (at the position of the 500th), and an acceptable watermark detection threshold T_z is adaptively determined using the following equation:

$$T_s = \mu + k\sigma, \tag{9}$$

where μ and σ are the mean value and standard deviation of the 10,000 NC values, calculated by correlating the watermark with 10,000 random sequences, respectively. In our experiments, the μ of Lu and Liao's and the proposed method are about 0 and 0.25, respectively, and the σ are about 0.07 and 0.1, respectively. Assume that these 10,000 NC values are normally distributed. Let $f(x)$ be a normal probability density function. To make the probability of

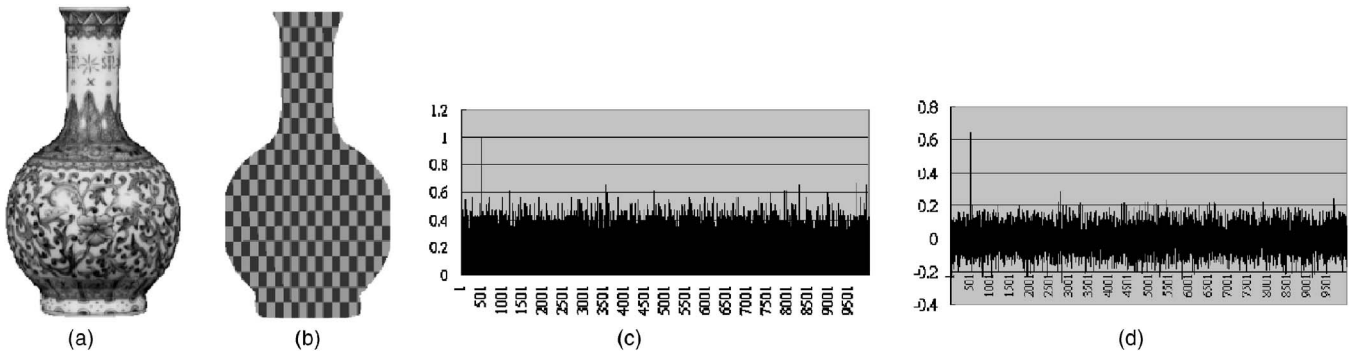

Fig. 4 Proposed scheme applied to the "Vase" object. (a) The test object image. (b) The shape subdivision of the image in (a). (c) The corresponding detector response using the proposed method. (d) The corresponding detector response using Lu and Liao's method.

false alarm less than ρ, the value of T_z must satisfy the following inequality:

$$\int_{T_z}^{\infty} f(x)\mathrm{d}x \leq \rho, \tag{10}$$

where

$$f(x) = \frac{1}{\sqrt{2\pi}\,\sigma} \exp\left[-\frac{(x-\mu)^2}{2\sigma^2}\right].$$

In our experiments, the value 4.265 of k is determined to make the probability of a false positive of a random watermark less than 10^{-5}. The threshold values of T_z for Lu and Liao's method and the proposed method are 0.3 and 0.68, respectively. The experimental results of several kinds of attacks using these two methods are shown in Table 1. A study of the threshold selection for correlation can be found in Ref. 21.

5 Discussion

Digital watermarking algorithms in the frequency domain are well known to resist general image-processing attacks better than those in the spatial domain. The experimental results also show that Lu and Liao's method performed

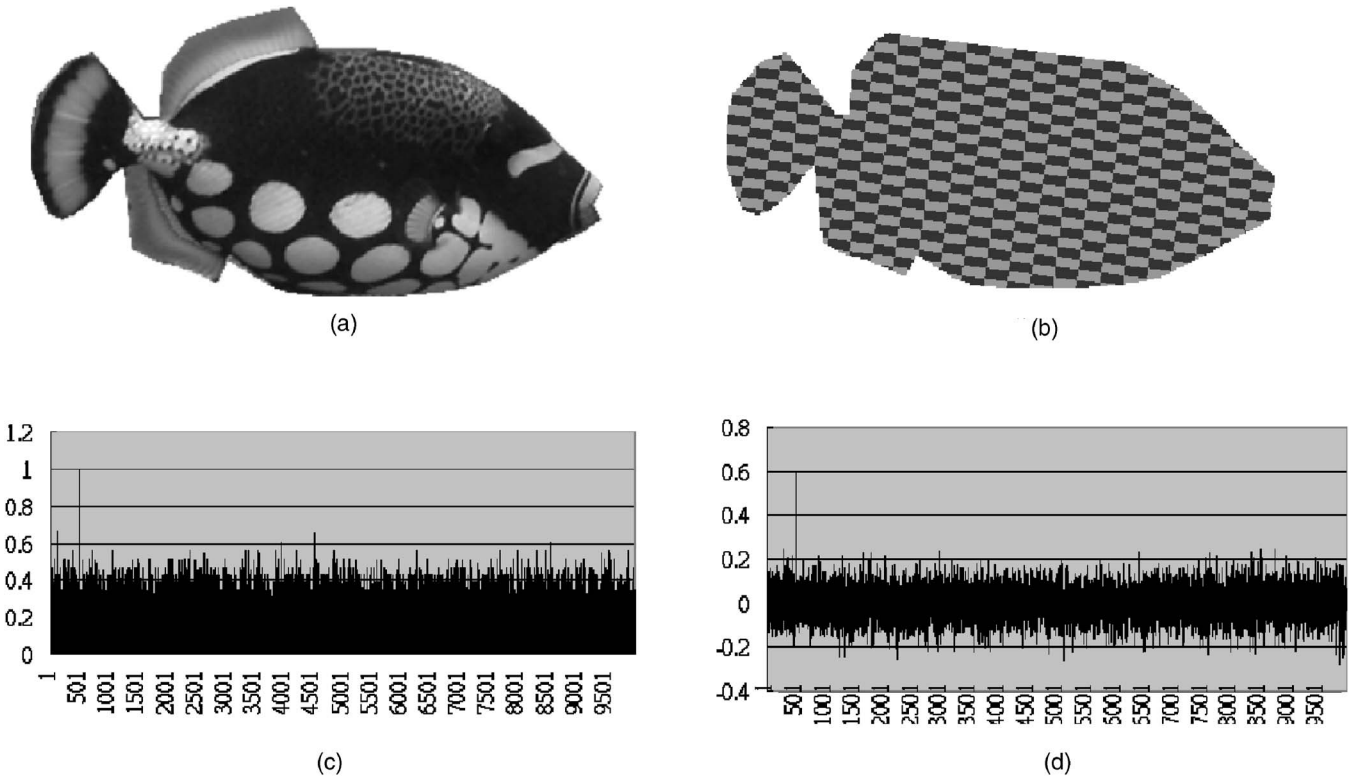

Fig. 5 Proposed scheme applied to the "Fish" object. (a) The test object image. (b) The shape subdivision of the image in (a). (c) The corresponding detector response using the proposed method. (d) The corresponding detector response using Lu and Liao's method.

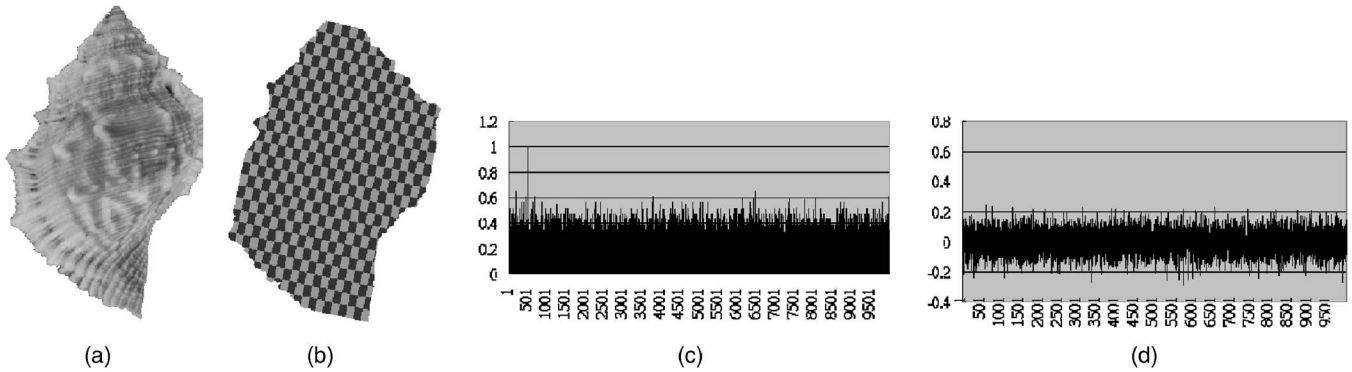

Fig. 6 Proposed scheme applied to the "Sea Shell" object. (a) The test object image. (b) The shape subdivision of the image in (a). (c) The corresponding detector response using the proposed method. (d) The corresponding detector response using Lu and Liao's method.

slightly better than the proposed method in some image-processing attacks, such as mean filtering and uniform noise addition. However, the proposed method performed much better than that of Lu and Liao in resisting general geometrical attacks such as row or column removal. In addition, we assume that the parameters of the affine transformation (rotation and scaling) attacks in Lu and Liao's method are known, so we can reconstruct the original shape

Table 1 Experimental results on robustness against attacks.

	NC							
Target object image:	"Russian Doll"		"Vase"		"Fish"		"Sea Shell"	
Method:	Ours	Ref. 16	Ours	Ref. 16	Ours	Ref. 16	Ours	Ref. 16
PSNR:	38.20	41.39	39.26	39.55	39.96	39.37	38.02	43.31
Watermarked (no attack)	1.00	0.80	1.00	0.64	1.00	0.59	1.00	0.69
Mean filter								
3×3	0.88	0.80	0.94	0.66	0.82	0.63	1.00	0.69
5×5	0.88	0.80	0.94	0.68	0.82	0.63	0.71	0.70
IPEG (20%)	0.94	0.58	0.94	0.16[a]	0.72	0.57	0.94	0.02[a]
Uniform								
$\sigma=10$	1.00	0.80	1.00	0.64	1.00	0.59	1.00	0.68
$\sigma=15$	0.94	0.80	0.35[a]	0.64	0.88	0.59	1.00	0.68
$\sigma=20$	0.94	0.80	0.18[a]	0.64	0.35[a]	0.58	0.94	0.67
Rotation (20 deg.)	1.0	0.72	0.92	0.62	0.82	0.59	1.00	0.14[a]
Scaling:								
0.8×0.8	0.88	0.72	0.88	0.64	0.82	0.59	0.94	0.69
0.9×0.9	0.94	0.72	0.94	0.62	0.88	0.59	1.00	0.69
1.1×1.1	0.88	0.72	1.0	0.62	0.72	0.59	0.94	0.69
One row or column removal	1.00	0.20[a]	1.0	0.45	0.94	0.11[a]	1.00	0.15[a]
Two rows or columns removal	0.92	0.05[a]	1.0	0.21[a]	0.88	0.09[a]	0.88	0.14[a]

[a]Undetectable.

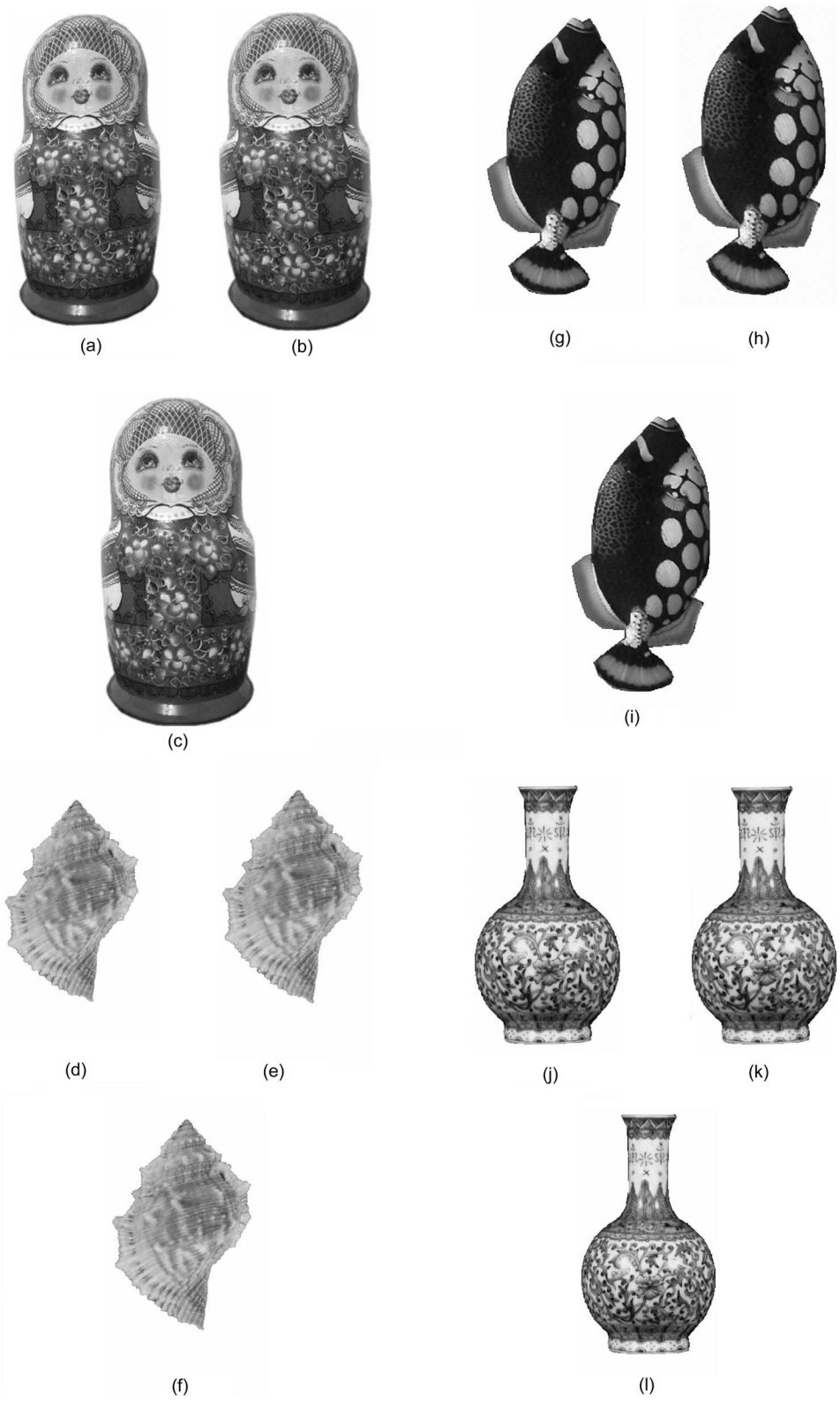

Fig. 7 Distortion results using StirMark and their corresponding BER and NC values by using the proposed method. "Russian Doll:" (a) affine transform (BER=3/32; NC=0.82); (b) random distortion (BER=5/32; NC=0.71); (c) line removal (BER=3/32; NC=0.82). "Sea Shell:" (d) affine transform (BER=3/32; NC=0.82); (e) random distortion (BER=2/32; NC=0.88); (f) line removal (BER=0; NC =1). "Fish:" (g) affine transform (BER=4/32; NC=0.76); (h) random distortion (BER=5/32; NC =0.70); (i) line removal (BER=2/32; NC=0.88). "Vase:" (j) affine transform (BER=5/32; NC=0.71); (k) random distortion (BER=5/32; NC=0.71); (l) line removal (BER=3/32; NC=0.82).

before performing watermark detection. Therefore, the experimental results seem to be good in these cases. In practical applications, however, Lu and Liao's method will suffer from the resynchronization problem, since those parameters are in fact unknown.

Furthermore, certain commercial software applications, including PhotoImpact and PhotoShop, provide a boundary-pixel cropping function to erode the boundary pixels of object images. Row or column removal and boundary-pixel cropping attacks will change the image dimensions. Without the information of the original image dimensions, any DCT-based method will fail in watermark detection. Besides, after some geometrical attacks such as affine transformation and random distortion, since the DCT coefficients are sensitive to geometrical distortion, the embedded watermark is still difficult to detect even if the dimensions of the original image have been recorded.

To evaluate the effectiveness of the proposed method, some geometrically distorted results generated by the StirMark benchmark tool are used for testing. These distortions include affine transformation, random distortion, and the removal of a large number of lines. Experimental results illustrated in Fig. 7 showed that the proposed method is quite effective in resisting these attacks. The bit error rate (BER) was used to measure the similarity between the K-bit pattern $v=(v_0,v_1,\ldots,v_{k-1})$ and the original watermark w:

$$\mathrm{BER}=\frac{|\{v_j:v_j\neq w_j\}|}{K}.$$

The NC values shown in Table 1 are all larger than the thresholds T_z of 0.68. These results show our method to be successful in watermark detection.

We also applied these attacks to Lu and Liao's method. Since the DCT-based methods are quite sensitive to geometrical distortion, without knowing the degree of distortion as side information, the NC values obtained using Lu and Liao's method are all in the range $(-0.1,0.1)$ and are undetectable.

Segmenting an object from an image could be fatal to watermark detection using a non-object-based watermarking approach.[22] The proposed object-based watermarking scheme can select relevant objects separately and embed watermarks into the selected objects. These objects should be the most important components of the image. When a certain region containing one of these objects is cut from the image and poached, the watermarks should still be detected accurately with the proposed method. Figure 8 shows an example of embedding watermarks into a selected object, namely the face "Lena." The experimental result indicates that a high NC value of 0.82 is obtained even following rotation, scaling, and boundary-pixel cropping attacks.

Moreover, the proposed scheme can efficiently achieve the synchronization recovery that is required for recovering from some geometrical attacks, such as skew, when performing simple operations in shape subdivision. The skew operation changes the locations of the principal axes of image objects. Figure 9 shows an example of synchronization recovery from skewing the image "Vase." The x and y axes in Fig. 9(c) represent the orientation adjustment of the two principal axes. The output values on the z axis are the NC values of watermark detection. The maximum NC value indicates the accurate angular magnitude of skewing.

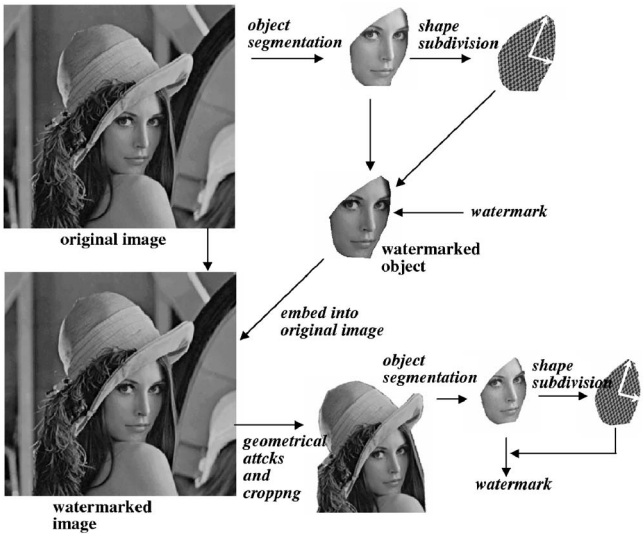

Fig. 8 An interactive object watermarking application using the proposed scheme.

The execution performance of the proposed algorithm is very good. It only has a time complexity of $O(M\times N)$ to embed or extract watermark bits in an image with size $M\times N$, since the major operations, including finding principal axes, pixel grouping, and gradient computation, all have $O(M\times N)$ time complexity. The execution times of the proposed method for an image of size 300×600 on a PC with 3-GHz CPU and 1-Gbit memory are 0.18 and 0.11 s for watermark embedding and extraction, respectively.

6 Conclusions

This study has presented a new object-based watermarking method, based on efficient segmentation, using parallel and perpendicular lines, of two principal axes in the spatial domain. This proposed scheme also was compared with the DCT-based method developed by Lu and Liao. Four object images taken from product images on the eBay auction Web site were adopted for model testing. Experimental results indicate that the proposed scheme resists geometrical attacks more effectively than that of Lu and Liao. The proposed method was also applied to an object image cut from

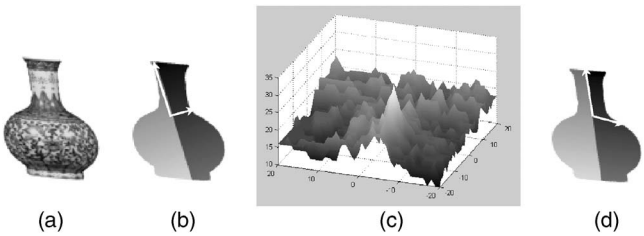

Fig. 9 An experiment on skew calibration by searching for the nearby angles of computed principal-axis orientations. (a) The skewed "Vase" image. (b) The principal-axis detection for the object in (a). (c) Synchronization recovery by searching for correct orientations of the two principal axes. (d) The principal axes after recovery.

the "Lena" image, which was then pasted back, and the object was cut again for watermark detection. Results of this study demonstrate that multiple objects in an image might be watermarked on demand by using the proposed method.

Acknowledgments

The authors would like to thank the National Science Council of the Republic of China, Taiwan, for financially supporting this research under contract No. NSC93-2213-E-006-051.

References

1. W. Bender, D. Gruhl, N. Morimoto, and A. Lu, "Techniques for data hiding," *IBM Syst. J.* **35**(3&4), 313–336 (1996).
2. C.-T. Hsu and J.-L. Wu, "Hidden signatures in images," in *Proc. Int. Conf. on Image Processing*, pp. 223–226, IEEE (1996).
3. L. M. Marvel, C. G. Boncelet, and C. T. Retter, "Spread spectrum image steganography," *IEEE Trans. Image Process.* **8**(8), 1075–1083 (1999).
4. I. J. Cox, J. Kilian, F. T. Leighton, and T. Shamoon, "Secure spread spectrum watermarking for multimedia," *IEEE Trans. Image Process.* **6**, 1673–1687 (1997).
5. V. Solachidis and I. Pitas, "Circularly symmetric watermark embedding in 2-D DFT domain," *IEEE Trans. Image Process.* **10**(11), 1741–1753 (2001).
6. H. Inoue, A. Miyazaki, A. Yamamoto, and T. Katsura, "A digital watermark based on wavelet transform and its robustness on image processing," in *Proc. Int. Conf. on Image Processing*, Vol. 2, pp. 391–395, IEEE (1998).
7. P. Bas, J.-M. Chassery, and F. Davoine, "Using the fractal code to watermark images," in *Proc. Int. Conf. on Image Processing*, Vol. 1, pp. 469–473, IEEE (1998).
8. V. Solachidis and F. M. Boland, "Phase watermarking of digital images," in *Proc. Int. Conf. on Image Processing*, Vol. 3, pp. 239–242, IEEE (1996).
9. P. Bas, J.-M. Chassery, and B. Macq, "Geometrically invariant watermarking using feature points," *IEEE Trans. Image Process.* **11**(9), 1014–1028 (2002).
10. I. J. Cox, M. L. Miller, and J. A. Bloom, *Digital Watermarking*, Morgan Kaufmann Publishers, San Francisco (2002).
11. M. Wu, M. L. Miller, J. A. Bloom, and I. J. Cox, "A rotation, scale and translation resilient public watermark," in *IEEE Conf. ICASSP'99*, Vol. 4, p. 2065 (1999).
12. C. Y. Lin, M. Wu, A. Bloom, I. J. Cox, M. L. Miller, and Y. M. Lui, "Rotation, scaling and translation resilient watermarking for images," *IEEE Trans. Image Process.* **10**(5), 767–782 (2001).
13. M. D. Swanson, B. Zhu, B. Chau, and A. H. Tewfik, "Object-based transparent video watermarking," in *IEEE Workshop on Multimedia Signal Processing*, pp. 369–374 (1997).
14. A. Piva, R. Caldell, and A. D. Rosa, "A DWT-based object watermarking system for MPEG-4 video streams," in *IEEE Int. Conf. on Image Processing*, Vol. 3, pp. 5–8 (2000).
15. H. Guo and P. F. Shi, "Object-based watermarking scheme robust to object manipulations," *Electron. Lett.* **38**(25), 1656–1657 (2002).
16. C. S. Lu and H. Y. M. Liao, "Video object-based watermarking: a rotation and flipping resilient scheme," in *Proc. Int. Conf. on Image Processing*, Vol. 2, pp. 483–486 (2001).
17. M. Y. Wu and Y. K. Ho, "A robust object-based watermarking scheme based on shape self-similarity segmentation," in *5th Int. Symp. on Multimedia Software Engineering*, pp. 110–113, IEEE (2003).
18. F. A. P. Petitcolas, R. J. Anderson, and M. G. Kuhn, "Attacks on copyright marking systems," in *Information Hiding, Second Int. Workshop, IH'98, Proc.*, pp. 219–239, Springer-Verlag (1998).
19. F. A. P. Petitcolas, "Watermarking schemes evaluation," *IEEE Signal Process. Mag.* **17**(5), 58–64 (2000).
20. P. M. Chen, "Robust digital watermarking based on a statistic approach," in *2000 Int. Symp. on Information Technology (ITCC2000)*, pp. 116–121, IEEE Computer Soc. (2000).
21. A. Piva, M. Barni, F. Bartolini, and V. Cappellini, "Threshold selection for correlation based watermark detection," in *Proc. COST254 Workshop on Intelligent Communications*, pp. 67–72 (1998).
22. J. Dittmann, F. Neck, A. Steinmetz, and R. Steinmetz, "Interactive watermarking environments," in *IEEE Conf. on Multimedia Computing and Systems*, pp. 286–294 (1998).

Biographies and photographs of the authors not available.